01 Apr 2011

Hydrogen-Deuterium Isotope Shift: From the 1S-2s-Transition Frequency to the Proton-Deuteron Charge-Radius Difference

Ulrich D. Jentschura

Missouri University of Science and Technology, ulj@mst.edu

Arthur N. Matveev

Christian G. Parthey

Janis Alnis

et. al. For a complete list of authors, see https://scholarsmine.mst.edu/phys_facwork/836

Recommended Citation

U. D. Jentschura et al., "Hydrogen-Deuterium Isotope Shift: From the 1S-2s-Transition Frequency to the Proton-Deuteron Charge-Radius Difference," *Physical Review A - Atomic, Molecular, and Optical Physics*, vol. 83, no. 4, pp. 042505-1-042505-9, American Physical Society (APS), Apr 2011.

The definitive version is available at https://doi.org/10.1103/PhysRevA.83.042505

Hydrogen-deuterium isotope shift: From the 1S-2S-transition frequency to the proton-deuteron charge-radius difference

U. D. Jentschura,[1] A. Matveev,[2] C. G. Parthey,[2] J. Alnis,[2] R. Pohl,[2] Th. Udem,[2] N. Kolachevsky,[2,*] and T. W. Hänsch[2,†]
[1]*Department of Physics, Missouri University of Science and Technology, Rolla, Missouri 65409-0640, USA*
[2]*Max-Planck-Institut für Quantenoptik, DE-85748 Garching, Germany*
(Received 11 February 2011; published 12 April 2011)

We analyze and review the theory of the hydrogen-deuterium isotope shift for the 1S-2S transition, which is one of the most accurately measured isotope shifts in any atomic system, in view of a recently improved experiment. A tabulation of all physical effects that contribute to the isotope shift is given. These include the Dirac binding energy, quantum electrodynamic effects, including recoil corrections, and the nuclear-size effect, including the pertaining relativistic and radiative corrections. From a comparison of the theoretical result $\Delta f_{\rm th} = 670\,999\,566.90(66)(60)$ kHz (exclusive of the nonrelativistic nuclear-finite-size correction) and the experimental result $\Delta f_{\rm expt} = 670\,994\,334\,605(15)$ Hz, we infer the deuteron-proton charge-radius difference $\langle r^2\rangle_d - \langle r^2\rangle_p = 3.820\,07(65)$ fm^2 and the deuteron structure radius $r_{\rm str} = 1.975\,07(78)$ fm.

DOI: 10.1103/PhysRevA.83.042505 PACS number(s): 31.30.jf, 14.20.Dh, 13.40.−f

I. INTRODUCTION

The 1S-2S hydrogen-deuterium isotope shift is one of the most accurately measured isotope shifts in physics. Compilations of the contributing effects in the literature have been somewhat sketchy. Since the isotope shift is a primary source of information for the determination of the isotopic difference of the nuclear charge radii, such a compilation appears to be useful, not the least because of recently improved experiments. Our 2009 experiment [1] has recently confirmed the experimental value for the 1S-2S isotope shift reported in Ref. [2] and improved its accuracy by about an order of magnitude.

From a comparison of theory and experiment, it is possible to determine the mean-square charge-radius difference. Denoting the mean-square nuclear charge radius as $\langle r^2\rangle$, we remember that the leading-order energy shift $\Delta E_{\rm NS}$ (for S states) due to the nuclear-size effect is given by the expression (in SI units)

$$E_{\rm NS} = h f_{\rm NS} = \frac{2}{3}\left(\frac{m_r}{m_e}\right)^3 \frac{(Z\alpha)^4 m_e c^2}{n^3}\,\frac{\langle r^2\rangle}{\lambda\!\!\!^{-}_C{}^2}\,\delta_{\ell 0}\,, \tag{1}$$

where n is the principal quantum number of the atomic state. The physical quantities are denoted as usual: h is the Planck constant, α is the fine-structure constant, Z is the nuclear charge number ($Z = 1$ for proton and deuteron), m_r is the reduced mass of the system, m_e is the electron mass, m_N is the nuclear mass, c is the speed of light, and $\lambda\!\!\!^{-}_C = \hbar/(m_e c)$ is the Compton wavelength of the electron divided by a factor 2π. Equation (1) relates the electron "size" (its Compton wavelength) to the proton "size" (its charge radius). The Kronecker delta is nonvanishing only for S states with orbital angular momentum $\ell = 0$. The energy shift is $E_{\rm NS}$ and the corresponding frequency is $f_{\rm NS}$. Taking into account the fact that $\lambda\!\!\!^{-}_C \propto m_e^{-1}$, we note that $E_{\rm NS}$ is proportional to m_e^3, which provides the basis for an accurate determination of the nuclear charge radius using muonic atoms [3], where m_e is replaced by m_μ.

For reference purposes, we note that the proton radius is defined as follows:

$$\langle r^2\rangle_p = 6\hbar^2\,\frac{\partial G_E}{\partial q^2}\bigg|_{q^2=0}\,, \tag{2}$$

where G_E is the electric Sachs form factor of the proton, with radiative corrections [4–9] being subtracted.

For the isotope shift exclusive of the main nuclear-size effect, the following theoretical result has been given in Eq. (8) of Ref. [2], which reads as $\Delta f_{\rm th} = 670\,999\,568.6(1.5)(1.5)$ kHz. Here, the first uncertainty comes from the electron-proton mass ratio and the second is the theoretical uncertainty. In general, we here denote all physical quantities related to the hydrogen-deuterium isotope shift with a Δ, whereas contributions to the energy shifts of individual atomic energy levels are denoted without this prefix. In Eq. (399) of the extensive review article [10], we find the result $\Delta f_{\rm th} = 670\,999\,568.9(1.5)(0.8)$ kHz, where the first uncertainty is from the electron-proton mass ratio and the second is from a theoretical uncertainty due to uncalculated higher-order terms. It is stated in Sec. 16.1.6 of Ref. [10] that the theoretical uncertainty of the isotope shift is mainly determined by the unknown single logarithmic and nonlogarithmic contributions of order $(Z\alpha)^7\,(m/M)$ and $\alpha(Z\alpha)^6\,(m/M)$, and also by the uncertainties of the deuteron size and structure contributions. The overall theoretical uncertainty of all contributions to the isotope shift, exclusive of the leading proton and deuteron size corrections, is quoted as 0.8 kHz in Ref. [10].

Here, we reanalyze the effect in light of the most recent theoretical developments, and we also present a compilation of all contributing physical effects. Including a rather conservative estimate for the multiphoton exchange contribution to the nuclear polarization effect for the isotope shift, our theoretical result reads as

$$\Delta f_{\rm th} = 670\,999\,566.90(66)(60)\ \text{kHz}\,. \tag{3}$$

The first uncertainty is due to (recently improved) values of the electron-to-proton and electron-to-neutron mass ratios [11].

[*]Also at P. N. Lebedev Physical Institute, Moscow, Russia.
[†]Also at Ludwig-Maximilians-University, Munich, Germany.

The new values for these mass ratios are also the primary reason why the theoretical value given in Eq. (3) is slightly different from that used in Ref. [2] and in Sec. 16.1.6 of Ref. [10].

The difference $\Delta f_{\rm expt} - \Delta f_{\rm th}$ is due to the nuclear-size effect given in Eq. (1) and allows for a determination of the nuclear charge-radius difference $\langle r^2\rangle_d - \langle r^2\rangle_p$ based on atomic-physics experiments, as detailed below. From scattering experiments, on the other hand, one may determine nuclear-physics values for the charge radii. Based on a careful analysis of the world scattering data, the deuteron root-mean-square (rms) charge radius $r_d = \sqrt{\langle r^2\rangle_d}$ has been obtained in Ref. [12] as $r_d = 2.130(9)$ fm, where we have added the statistical and systematic uncertainties given in Ref. [12] quadratically. This value is in good agreement with the recommended value derived from the 2006 CODATA adjustment of the fundamental constants

$$r_d = 2.1402(28)\ \text{fm} \qquad (\text{Refs. [11,13]})\,. \tag{4}$$

As explained in Ref. [13], this value of the deuteron charge radius is mostly based on a theoretical analysis of the most accurately measured transition frequencies in hydrogen and deuterium.

An analysis of the world scattering data for the proton leads to a value of $r_p = 0.895(18)$ fm (Refs. [14–16]), which is in good agreement with the recommended value derived from the 2006 CODATA adjustment of the fundamental constants

$$r_p = 0.8768(69)\ \text{fm} \qquad (\text{Refs. [11,13]})\,. \tag{5}$$

The most recent value from electron scattering [17] reads as $r_p = 0.879(8)$ fm, where we quadratically add the statistical and systematic uncertainties given in Ref. [17]. The recent Lamb shift measurement in muonic hydrogen, however, leads to a value of

$$r_p = 0.841\,84(67)\ \text{fm} \qquad (\text{Ref. [3]})\,, \tag{6}$$

which is in disagreement with the two above-mentioned values from electron scattering values and with the 2006 CODATA value. The difference of the CODATA mean-square radii of deuteron and proton reads as

$$\langle r^2\rangle_d - \langle r^2\rangle_p = 3.812(17)\ \text{fm}^2 \qquad [\text{Eqs. (4) and (5)}]. \tag{7}$$

By contrast, the difference of the CODATA deuteron radius (4) and the muonic hydrogen proton radius (6) is $\langle r^2\rangle_d - \langle r^2\rangle_p = 3.872(12)\ \text{fm}^2$. One of the motivations for this paper is to verify if the difference of the CODATA charge radii of deuteron and proton is compatible with the measurement of the isotope shift. Another motivation is to fill a gap in the literature: the theory of the isotope shift has never been discussed in great detail, and a dedicated compilation of all effects that contribute to the shift is missing up to now.

A particular remark should be made. The 1997 isotope-shift measurement [2] is used as an input datum for the CODATA analysis [11], and one may thus wonder to which extent the measurement of the isotope shift and the concomitant determination of the deuteron-proton mean-square-radius difference is independent from the CODATA values of the mean-square radii of the individual nuclei. In the last two rows of Table XLV of Ref. [11], it is clarified that a separate comparison of transition frequencies in both hydrogen and deuterium to theory (without using the isotope shift as an input datum) leads to the values $r_p = 0.8802(80)$ fm and $r_d = 2.1286(93)$ fm, which are both in excellent agreement with the CODATA values given in Eqs. (4) and (5).

To address the current situation, we here discuss the theory of the isotope shift in detail. Calculations will be presented together with some information that is not readily accessible from the original literature references. Following our general outline, we first describe the advances in the experiment that have led to the recent improvements in the measurement of the isotope shift, before summarizing the current status of the theory of the isotope shift in Sec. III, describing all contributions. The nuclear charge-radius difference of proton and deuteron is evaluated in Sec. IV, based on the isotope shift. Finally, conclusions are drawn in Sec. V.

II. MEASUREMENT OF THE ISOTOPE SHIFT

The $1S$-$2S$ hydrogen-deuterium isotope shift was remeasured in the period from March 2009 to January 2010 by means of Doppler-free two-photon spectroscopy on a thermal atomic beam [1]. Here, we briefly discuss the main improvements of the measurement relative to the previous experiment conducted in 1997 (Ref. [2]).

The tenfold reduction of the uncertainty of the frequency difference $f^D_{1S\text{-}2S} - f^H_{1S\text{-}2S}$ in the 2010 measurement compared to the measurement in 1997 results from three factors: (i) implementation of a new all-solid-state ultrastable laser system, (ii) implementation of an optical frequency measurement based on an Er-doped fiber frequency comb, which allows higher data rates, and (iii) availability of more accurate input data for the determination of the hyperfine centroid frequency from the measured transition frequency, which involves specific hyperfine components.

These improvements will now be discussed. To this end, let us first review a few basic principles of the isotope-shift measurement by optical frequency comparison. Namely, in order to measure the difference of the $1S$-$2S$ transition frequencies in deuterium and hydrogen, we excite the hyperfine transitions $F = \frac{3}{2} \to \frac{3}{2}$, $m_F = \pm\frac{3}{2} \to \pm\frac{3}{2}$ in deuterium (D) and $F = 1 \to 1, m_F = \pm 1 \to \pm 1$ in hydrogen (H) and denote the isotope shift of the measured hyperfine structure (HFS) components as $\Delta f_{\rm DH}$. The choice is determined by their low sensitivity to magnetic fields because of their nearly equal Landé g factors (the $1S$ and the $2S$ Landé g factors differ only by relativistic corrections of order α^2). The isotope shift $\Delta f_{\rm expt}$ of the $1S$-$2S$ hyperfine centroid is given by the difference of the transition frequencies

$$\Delta f_{\rm expt} = f^{\rm D}_{1S\text{-}2S} - f^{\rm H}_{1S\text{-}2S} - \Delta f_{\rm HFS} \equiv \Delta f_{\rm DH} - \Delta f_{\rm HFS}, \tag{8a}$$

where $\Delta f_{\rm DH} = f^{\rm D}_{1S\text{-}2S} - f^{\rm H}_{1S\text{-}2S}$, and the hyperfine subcomponents are

$$f^{\rm D}_{1S\text{-}2S} \equiv f^{\rm D}_{1S\text{-}2S}\big(F = \tfrac{3}{2} \to \tfrac{3}{2}, m_F = \pm\tfrac{3}{2} \to \pm\tfrac{3}{2}\big)\,, \tag{8b}$$

$$f^{\rm H}_{1S\text{-}2S} \equiv f^{\rm H}_{1S\text{-}2S}\,(F = 1 \to 1\,, m_F = \pm 1 \to \pm 1)\,. \tag{8c}$$

We thus have to determine the hyperfine correction $\Delta f_{\rm HFS}$ to high accuracy. The optical measurements of the $2S$ hyperfine

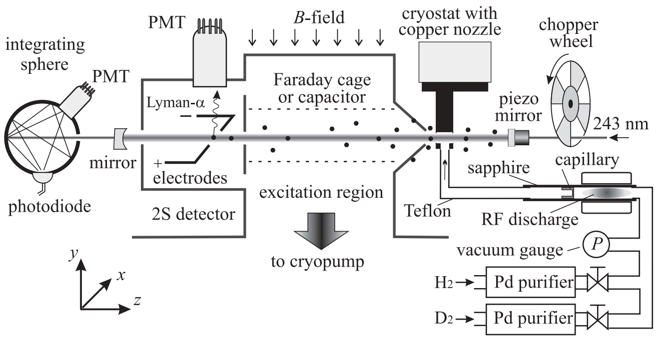

FIG. 1. Schematic of the excitation region. For the characterization of the dc Stark shift, the Faraday cage is replaced by a plane capacitor with the electric field oriented along one of the three axes (see also Fig. 3). PMT denotes a photomultiplier tube.

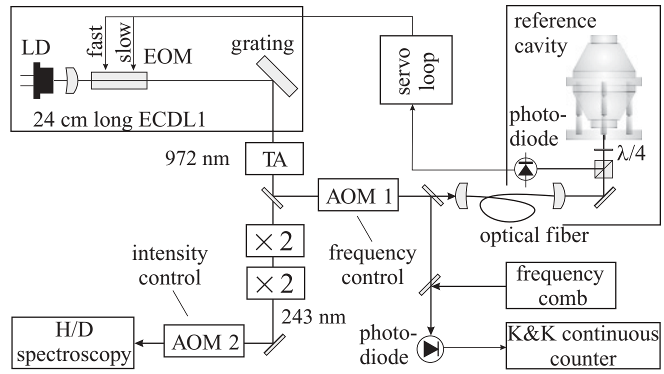

FIG. 2. Schematic of the long cavity laser system used for both isotopes. ECDL: extended cavity diode laser, LD: laser diode, EOM: electro-optical modulator, TA: tapered amplifier, and AOM: acousto-optic modulator.

intervals in H and D [18,19] together with the radio-frequency measurements of the ground-state splitting [20,21] give a result of $\Delta f_{\mathrm{HFS}} = 215\,225\,596.5(2.9)$ Hz. This is a factor of 4.5 more accurate than the value used in [2] due to the improved $2S$ interval frequencies as reported in Refs. [18,19].

The general experimental setup is given in Fig. 1 and follows the principle of time-resolved two-photon spectroscopy laid out in Ref. [22]: A 160-Hz light chopper with a 50% duty cycle is installed before the 243-nm enhancement cavity used for the time-of-flight measurements. After blocking the light, well-defined delay times $\tau = 10, 210, \ldots, 2210$ μs are implemented before the start of the detection of $2S$ atoms along the atomic beam line. The fastest $2S$ atoms escape, and the slowest atoms are selected from the initial distribution. Lines recorded at higher delays τ exhibit a smaller second-order Doppler effect as well as reduced time-of-flight broadening at the expense of lesser count rates since there are fewer atoms. To introduce the delay, we use a multichannel scaler that simultaneously records 12 delayed lines [23].

Each measurement day started from one of the two randomly chosen isotopes, for which we recorded up to 100 $1S$-$2S$ spectra during less than four hours. Then we readjusted the system for the other isotope and measured it in a similar way. The overall measurement time was restricted by the saturation of the cryogenic pump (see Fig. 1). Compared to the 1997 measurement, we replaced the one-directional scan over the $1S$-$2S$ transition by changing the laser frequency in a random order around the transition center. This reduces conceivable systematic effects (e.g., due to a slow change in the atomic flow as a function of time). At each laser frequency, we alternate between two power levels differing by typically a factor of 2. Thus, we simultaneously record two $1S$-$2S$ lines taken at different intensities, but otherwise similar conditions. This allows for a more accurate correction of the ac Stark shift as compared to the 1997 measurement.

The diode laser setup mainly used in the experiment [1] is schematically depicted in Fig. 2. We use an extended cavity diode laser (ECDL) at 972 nm with a 24-cm-long resonator in Littrow configuration with an intracavity electro-optical modulator (EOM). The laser is locked to a high-finesse ultralow expansion glass (ULE) cavity in vertical configuration maintained at the critical temperature at which the sensitivity of the cavity length to temperature fluctuations is minimal [24]. Locking to the cavity provides a spectrally narrow laser carrier (0.5 Hz) with a nearly linear frequency drift of only $+50$ mHz s^{-1}. This feature significantly simplifies the measurement of the instant laser frequency by a frequency comb.

To measure the frequency of the spectroscopy light, we use a 250-MHz repetition rate Er-doped fiber frequency comb. By beating part of the light sent to the reference cavity with the comb we disentangle the spectroscopic routine (scanning of the AOM and recording $1S$-$2S$ spectra) from the frequency measurement of the laser. In this case, the frequency measurement can be done with continuous counters (we use Klische+Kramer FX-80), and their frequency readings are separately saved together with time marks. Due to the very low drift of the ULE cavity, the time synchronization of counters and the laser-frequency scanning only has to be accurate on the order of a second. Such an approach typically allows us to accumulate twice as much frequency data compared to previous measurements, e.g., Ref. [25], and to define the instant laser frequency with less uncertainty.

As a frequency reference for the frequency comb, we use an active, GPS referenced hydrogen maser. The required fractional inaccuracy of the frequency reference is of the order of 10^{-11}, but should be very stable during the comparison of the isotopes (with a fractional instability of 10^{-15}). Indeed, the isotope shift is the difference of two big numbers $f^{\mathrm{D}}_{1S\text{-}2S}$ and $f^{\mathrm{H}}_{1S\text{-}2S}$, each of the order of 10^{15}Hz. According to its specification, the maser has a frequency instability lower than 2×10^{-15} within one day. The measurements of both isotopes should thus be done within one day. The GPS calibration, in turn, provides a frequency inaccuracy of 5×10^{-15}, which is not limiting.

Systematic effects have been discussed in Ref. [1]. Of particular importance is the estimate of the dc Stark effect due to conceivable stray fields. For fields along the x axis, the procedure for estimating the stray fields is illustrated in Fig. 3. Based on this estimate, we set an upper limit of $|E_{\mathrm{stray}}| < 6$mV/cm for stray fields along the axis. Repeating the measurement for all three axes and converting the stray field to a dc Stark frequency shift, we can finally set a limit of $\Delta f_{\mathrm{stray}} < 1$ Hz for the excitation volume restricted by the two diaphragms (Fig. 1). However, we can not probe the region

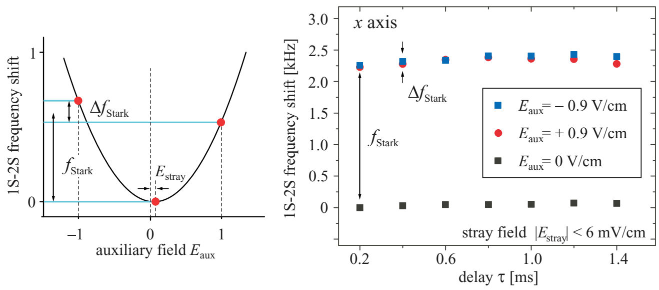

FIG. 3. (Color online) Characterization of the stray fields in the excitation region with the help of an auxiliary electric field $\pm E_{\rm aux}$ applied by a plane capacitor field along one of the axes x, y, and z. Measuring the transition frequency for an auxiliary field $\pm E_{\rm aux}$ and zero auxiliary field, we can fit a three-parameter parabola to the data. The deviation of the center of the parabola from the point recorded at zero auxiliary field then is a measure of the dc Stark shift due to stray fields. The probing of the stray fields along the x axis in our experimental setup is illustrated at the right part of the figure.

between the nozzle and the front diaphragm. Therefore, we conservatively assume the strength of a possible stray electric field there to be smaller than 100 mV/cm. For a delay of 1410μs, this corresponds to a line shift of 5 Hz, which we take as an uncertainty contributed by stray electric fields.

Due to irradiation with the 243-nm light, there is an ac Stark shift of the $1S$-$2S$ transition, the theoretical evaluation of which has been discussed in Refs. [22,26]. A difference between the isotopes can be caused only by errors in the power calibration, since the differential ac Stark shift for the $1S$-$2S$ transitions in H and D is negligible at our level of accuracy (it is caused mainly by the difference in the reduced masses of the two isotopes). We thus fit transition frequencies recorded at different powers by two lines with the same slope and add a 1 Hz uncertainty caused by the nonlinearity of our power calibration. Estimating the second-order Doppler shift at a typical delay of 1410 μs as described in Ref. [1] and adding an 11 Hz uncertainty due to a possible isotope-dependent pressure shift (the basis for this estimate has also been discussed in [1]), we finally obtain our uncertainty budget as given in Table I and the $1S$-$2S$ isotope shift as

$$\Delta f_{\rm expt} = 670\,994\,334\,605(15)\ {\rm Hz}\,, \tag{9}$$

which is a tenfold improvement over the 1997 result [2].

III. THEORY OF THE ISOTOPE SHIFT

A. Classification of corrections

The hydrogen-deuterium isotope shift of the hyperfine centroid of the $1S$-$2S$ transition, either measured experimentally or calculated theoretically, is denoted as

$$\Delta E_{\rm iso} = E(2S-1S)|_{\rm D} - E(2S-1S)|_{\rm H} = h\,\Delta f_{\rm iso}. \tag{10}$$

This is a positive quantity in the chosen convention ("deuterium minus hydrogen") because deuterium has a larger mass, and the reduced mass of the atomic deuterium system is slightly larger. Consequently, the $1S$-$2S$ transition frequency is slightly larger in deuterium than in hydrogen. The experimental result $\Delta f_{\rm expt}$ for the isotope-shift frequency $\Delta f_{\rm iso}$ is given in Eq. (9). The theoretical expression for $\Delta f_{\rm iso}$ is the

TABLE I. Results of the $1S$-$2S$ hydrogen-deuterium frequency measurements ($f^{1997}_{\rm expt}$, $f^{2010}_{\rm expt}$) and uncertainty budgets ($\sigma^{1997}_{\rm expt}$, $\sigma^{2010}_{\rm expt}$) for the 1997 (Ref. [2]) and 2010 (Ref. [1]) measurements, respectively. Contributions neglected in the 1997 measurement are denoted by dashes. The frequency $\Delta f_{\rm DH}$ is the HFS subcomponent defined in Eq. (8).

Contribution	$f^{1997}_{\rm expt}$ (Hz)	$\sigma^{1997}_{\rm expt}$ (Hz)	$f^{2010}_{\rm expt}$ (Hz)	$\sigma^{2010}_{\rm expt}$ (Hz)
$\Delta f_{\rm DH} - 671\,209\,560$ kHz	225	$\simeq 150$	203.1	5.1
$\Delta f_{\rm HFS} - 215\,225\,000$ Hz	585	14	596.5	2.9
ac Stark shift	–	–	0	1
dc Stark shift	–	–	0	5
Second-order Doppler	0	20	0	6
Density effects	–	–	0	11
$\Delta f_{\rm expt} - 670\,994\,334\,000$ Hz	640	150	606	15

sum of $\Delta f_{\rm th}$ given in Eq. (3) and of the main nuclear-size effect $\Delta f_{\rm NS}$, which corresponds to Eq. (1), evaluated for the isotope difference. As detailed below, the evaluation of $\Delta f_{\rm th}$ can be broken down as follows:

$$\Delta f_{\rm th} = \Delta f_{\rm i} + \Delta f_{\rm ii} + \Delta f_{\rm iii}\,, \tag{11}$$

where the three frequencies $\Delta f_{\rm i}$, $\Delta f_{\rm ii}$, and $\Delta f_{\rm iii}$ correspond to different sets of physical effects.

For an individual atomic level, the frequency $f_{\rm NS}$ corresponding to the finite-size effect given in Eq. (1) is positive. However, when evaluated for the isotope shift, the quantity $\Delta f_{\rm NS}$ given by

$$\Delta f_{\rm NS} = f_{\rm NS}(2S-1S)|_{\rm D} - f_{\rm NS}(2S-1S)|_{\rm H} \tag{12}$$

is negative. Indeed, the finite-size effect shifts energy levels upward by a shift proportional to $1/n^3$. This upward shift of the lower level (ground state) involved in the transition decreases the $1S$-$2S$ frequency in deuterium and therefore leads to a negative contribution to the finite-size term in the isotope shift defined in Eq. (12).

The following physical effects contribute to the isotope shift: Set (i). Difference in the Dirac energy and Barker-Glover [27] corrections. This difference depends on the electron-to-proton and electron-to-deuteron mass ratios. Set (ii). Difference in the Lamb shifts, and difference in the radiative-recoil corrections, which directly depend on the electron-to-nuclear-mass ratio. Approximately, this ratio is 1/2000 for hydrogen, but 1/4000 for deuterium. Set (iii). Higher-order corrections to the nuclear-size effect (third Zemach moment of the nuclear charge distribution, relativistic corrections, and self-energy and vacuum-polarization corrections to the finite-size effect). These effects depend on the mean-square charge-radii difference, but their absolute magnitude is small enough so that they can be evaluated to sufficient accuracy based on existing data for the charge radii. Set (iv). Difference in the main, leading, nonrelativistic nuclear-size effect as given in Eq. (12). Currrently, the most powerful way of analyzing the experiment lies in first evaluating corrections (i), (ii), and (iii), and then using the results to obtain the difference in the mean-square charge radii.

B. Fundamental constants

Let us briefly discuss the physical constants, mass ratios, and the corresponding uncertainties that are useful for the analysis of the isotope shift. According to Ref. [11], the electron-proton mass ratio is

$$\frac{m_e}{m_p} = 5.446\,170\,217\,7(24) \times 10^{-4} \tag{13}$$

with a relative uncertainty of 4.3×10^{-10}. The electron-deuteron mass ratio is

$$\frac{m_e}{m_d} = 2.724\,437\,109\,3(12) \times 10^{-4} \tag{14}$$

with a relative uncertainty of 4.2×10^{-10}. We also record the deuteron-proton mass ratio

$$\frac{m_d}{m_p} = 1.999\,007\,501\,08(22)\,. \tag{15}$$

Its relative uncertainty is 2.0×10^{-10}. For the fine-structure constant, we use the value from Ref. [28], which reads as

$$\alpha^{-1} = 137.035\,999\,084(51) \tag{16}$$

with a relative uncertainty of 6.9×10^{-10}. This value is consistent with the latest photon recoil measurement reported in Ref. [29]. The Rydberg constant, expressed in frequency units, is

$$R_\infty c = 3.289\,841\,960\,361(22) \times 10^{15}\ \text{Hz}\,. \tag{17}$$

Of these input data, only the Rydberg constant has sufficient relative accuracy (6.6×10^{-12}) to match the experimental result given in Eq. (9). Fortunately, the Rydberg constant can be factored out in the theoretical calculations [see Eq. (19) below]. The value of the $1S$-$2S$ transition is roughly given as

$$f_{1S\text{-}2S} \approx \frac{3}{4}\, R_\infty\, \frac{m_r}{m_e}\,. \tag{18}$$

Here, $m_r/m_e = 1/(1 + r_N)$ is the ratio of the reduced mass of the system to the electron mass ($r_N = m_e/m_N$ is the electron-nucleus mass ratio). A simple Taylor expansion in powers of r_N reveals that the shift $\Delta f_{1S\text{-}2S,N}$ of the $f_{1S\text{-}2S}$ transition frequency due to reduced-mass effect can be expressed roughly as

$$\Delta f_{1S\text{-}2S,N} \approx -\frac{3}{4}\, R_\infty\, r_N\,. \tag{19}$$

Consequently, the uncertainty $\delta f_{1S\text{-}2S}$ due to the mass ratios is

$$\begin{aligned}\delta f_{\text{iso},N} &= \frac{3}{4}\, R_\infty \left\{ \sqrt{\left[\delta\left(\frac{m_e}{m_d}\right)\right]^2 + \left[\delta\left(\frac{m_e}{m_p}\right)\right]^2} \right\}, \\ &= 662.0\,\text{Hz}\end{aligned} \tag{20}$$

for the isotope shift defined in Eq. (10). One may express the reduced-mass correction in terms of other mass ratios involved in the experiment (such as the proton-to-deuteron mass ratio), but the final uncertainty is invariant. While Eq. (19) is not sufficiently precise in order to predict the reduced-mass correction to the full isotope shift, it can nevertheless be used to estimate the uncertainty of the final result due to the uncertainty in the mass ratios. In general, the theoretical uncertainty in the isotope shift due to the mass ratios exceeds the experimental uncertainty recorded in Eq. (10) by a factor of 60.

One might question whether it is permissible to use a value of the Rydberg constant that is derived using the experimental value of the hydrogen $1S$-$2S$ frequency, as input for the theoretical analysis of the $1S$-$2S$ hydrogen-deuterium isotope shift. However, this question may easily be addressed. Namely, for our theoretical analysis, we need the Rydberg constant only up to an accuracy of about 10^{-10} to match the accuracy given for our theoretical value in Eq. (3). At this level of accuracy, we may refer to a completely independent determination of the Rydberg constant [30] via high-precision spectroscopy of Rydberg states of hydrogen, in agreement with Eq. (17), where a value of the Rydberg constant of relative accuracy 2.0×10^{-11} is obtained without any recourse to the $1S$-$2S$ frequency.

C. Evaluation of the corrections

Set (i). We first investigate the Dirac theory contribution to the isotope shift. (For the classification of the corrections, see Sec. III A.) According to Dirac theory, the energy level of a two-particle system consisting of an infinitely heavy nucleus and an orbiting electron of mass m_e, with the rest mass subtracted, is given as

$$\begin{aligned}E &= m_e c^2[f(n,j) - 1] = m_e c^2 \left[\frac{1}{\sqrt{1 + \epsilon(n,j)}} - 1\right], \\ \epsilon(n,j) &= \frac{(Z\alpha)^2}{\left[n - j - \frac{1}{2} + \sqrt{\left(j + \frac{1}{2}\right)^2 - (Z\alpha)^2}\right]^2}.\end{aligned} \tag{21}$$

Let us now define

$$g(\epsilon) \equiv \frac{1}{\sqrt{1+\epsilon}} - 1 = -\frac{\epsilon}{\sqrt{1+\epsilon}\,(1 + \sqrt{1+\epsilon})}\,. \tag{22}$$

Excluding Lamb shift and hyperfine effects, but including reduced-mass corrections, the bound-state energy of the two-body Coulomb system is given by [31]

$$\begin{aligned}E_{nj} &= m_r[f(n,j) - 1] - \frac{m_r^2}{2(m_e + m_N)}[f(n,j) - 1]^2, \\ &= m_e c^2 \left\{ \frac{1}{1 + r_N}\, g(\epsilon(n,j)) \right. \\ &\qquad \left. - \frac{r_N}{2(1 + r_N)^3}\, [g(\epsilon(n,j))]^2 \right\},\end{aligned} \tag{23}$$

where r_N again denotes the electron-to-nucleus mass ratio. This formula leaves the (n,j) degeneracy of the levels intact. The representation on the right-hand side of Eq. (23) has the additional advantage that the Rydberg constant can easily be factored out. Indeed, the frequency corresponding to E_{nj} is

$$f_{nj} = \frac{2\,E_{nj}}{\alpha^2 m_e c^2}\, R_\infty c\,. \tag{24}$$

The analytic cancellation of the $\alpha^2 m_e c^2$ factor in the first ratio (in curly brackets) is immediate if we consider the definition of $g(\epsilon)$ given in Eq. (22). The Barker-Glover corrections [27] follow from the two-body Breit Hamiltonian

$$E_{\rm BG} = \frac{(Z\alpha)^4 m_r^3}{2n^3 m_N^2}\left(\frac{1}{j+1/2} - \frac{1}{\ell+1/2}\right)(1-\delta_{\ell 0}), \quad (25)$$

but they vanish for S states. The term proportional to $\delta_{\ell 0}$ in Eq. (25) is the Darwin-Foldy (DF) term

$$\begin{aligned} E_{\rm DF} &= -\frac{(Z\alpha)^4 m_r^3 c^2}{2n^3 m_N^2}\left(\frac{1}{j+1/2} - \frac{1}{\ell+1/2}\right)\delta_{\ell 0}, \\ &= \frac{(Z\alpha)^4 m_r^3 c^2}{2n^3 m_N^2}\,\delta_{\ell 0}, \quad (26) \\ &= \frac{2}{3}\left(\frac{m_r}{m_e}\right)^3 \frac{(Z\alpha)^4 m_e c^2}{n^3 \lambda\!\!\!^{-}_C{}^2}\left(\frac{3\hbar^2}{4m_N^2 c^2}\right)\delta_{\ell 0}, \end{aligned}$$

which is due to the Zitterbewegung term of the nucleus [32]. A comparison of Eqs. (26) and (1) reveals that the Darwin-Foldy correction can be compensated by an addition to the mean-square nuclear charge radius according to

$$\langle r^2\rangle \to \langle r^2\rangle + \frac{3\hbar^2}{4m_N^2 c^2}\,. \quad (27)$$

In Ref. [33], the authors advocate to change the conventions for the proton charge radius such as to include the Darwin-Foldy term into $\langle r^2\rangle_p$. This convention is not followed here, and it also is not used in Refs. [2,11].

For non-S states, the Barker-Glover corrections lead to a numerically small violation of the (n,j) degeneracy. For hydrogen and deuterium S states, using the input data for the mass ratios given in Sec. III B, we obtain

$$\Delta f_{\rm i} = 671\,004\,071.29(66)\ \text{kHz} \quad (28)$$

for the Dirac contributions to the isotope shift, where the subscript i is inspired by the identification of the corrections in Sec. III A. The uncertainty of 0.66 kHz is due to the mass ratios given in Eqs. (13) and (14); the uncertainty induced by the fine-structure constant is negligible because we are expressing all quantities in terms of the Rydberg constant.

Set (ii). We now turn to set (ii) of the correction according to the classification presented in Sec. III A. These are Lamb shift contributions to the isotope shift. The relevant results are as follows. For the isotope shift due to the one-loop self-energy and vacuum polarization [see Eqs. (19)–(26) of Ref. [11]], we obtain

$$\Delta\nu_1 = -5558.99\ \text{kHz}\,. \quad (29)$$

The isotope shift due to two-loop self-energy and vacuum polarization and combined effects reads as, according to Eqs. (29)–(46) of Ref. [11],

$$\Delta\nu_2 = -0.51\ \text{kHz}\,. \quad (30)$$

Due to three-loop self-energy and vacuum polarization and combined effects, we calculate, according to Eqs. (47)–(49) of Ref. [11],

$$\Delta\nu_3 = -0.001\ \text{kHz}\,. \quad (31)$$

Isotope-shift effects due to the Salpeter recoil correction [34] given in Eqs. (11) and (12) of Ref. [11] sum up to

$$\Delta\nu_4 = 1032.65\ \text{kHz}\,. \quad (32)$$

The isotope shift due to the higher-order pure recoil terms [Eq. (13) of Ref. [11]] is given as

$$\Delta\nu_5 = -3.41(32)\ \text{kHz}\,. \quad (33)$$

The uncertainty estimate is due to an unknown higher-order pure recoil term of order $(Z\alpha)^7\ \ln(Z\alpha)\,(m_e/m_N)$:

$$\delta E_5 = (Z\alpha)^7\ \ln[(Z\alpha)^{-2}]\,\frac{m_r^3}{m_e^2\, m_N}\,\frac{m_e c^2}{n^3}\,, \quad (34)$$

for which we assume a unit prefactor. This estimate of the prefactor seems reasonable on the basis of the trend of the coefficients of lower order for the recoil effect.

Radiative-recoil terms [see Eqs. (11)–(16) of Ref. [11]] contribute

$$\Delta\nu_6 = -5.38(11)\ \text{kHz}\,. \quad (35)$$

Here, the uncertainty estimate is due to an unknown radiative-recoil term of order

$$\delta E_6 = \frac{\alpha}{\pi}(Z\alpha)^6\ \ln[(Z\alpha)^{-2}]\,\frac{m_r^3}{m_e^2\, m_N}\,\frac{m_e c^2}{n^3}\,, \quad (36)$$

for which we again assume a unit prefactor.

Note that the theoretical result for $\Delta\nu_6$ is valid provided the following result for the radiative-recoil correction E_6 to the energy levels is used:

$$E_6 = \frac{m_r^3}{m_e^2 m_N}\,\frac{\alpha(Z\alpha)^5}{\pi^2 n^3} m_e c^2 \delta_{\ell 0}\left[6\,\zeta(3) - 2\,\pi^2\ln 2 + \frac{35\,\pi^2}{36} - \frac{448}{27} + \frac{2}{3}\pi(Z\alpha)\,\ln^2(Z\alpha)^{-2} + \ldots\right]. \quad (37)$$

The nonlogarithmic contribution is the sum of two results; the first is obtained in Refs. [35,36] for the electron-line contribution, and the second is obtained in Ref. [37] for the vacuum-polarization term. The result listed here in Eq. (37) agrees with the numerical value given first in Ref. [38] for the entire set of radiative-recoil corrections of order $\alpha(Z\alpha)^5(m_e/m_N)$ (sum of electron line and vacuum polarization). The logarithmic contribution in Eq. (37) is obtained in Refs. [39,40]. The radiative-recoil correction of order $\alpha(Z\alpha)^5(m_e/m_N)$ has been the subject of rather intensive investigations [41–43] before agreement was reached with respect to the numerical value of the correction.

The nuclear self-energy given in Eq. (57) of Ref. [11] leads to a contribution of

$$\Delta\nu_7 = 2.98(10)\ \text{kHz}\,. \quad (38)$$

Due to muonic and hadronic vacuum polarization [Eqs. (27) and (28) of Ref. [11]], a tiny contribution of

$$\Delta\nu_8 = 0.006\ \text{kHz} \quad (39)$$

is obtained. According to Eqs. (17) and (18) of Ref. [11], the isotope shift due to nuclear polarizability reads as

$$\Delta\nu_9 = 18.64(2)\ \text{kHz}\,. \quad (40)$$

This value is based on the theoretical calculations of Refs. [44–47]. In view of the absence of the Zitterbewegung term for spin-1 nuclei (e.g., the deuteron, see Ref. [48]), we have an additional contribution to the bound-state energy for deuterium energy levels, which, for S states, reads as

$$\Delta E = -\frac{1}{2}\left(\frac{m_r}{m_N}\right)^2 \frac{(Z\alpha)^4 m_r c^2}{n^3}\delta_{\ell 0}\,. \tag{41}$$

This term is the negative of the Darwin-Foldy correction given in Eq. (26), as it is absent for deuterium energy levels. The corresponding contribution to the isotope shift

$$\Delta\nu_{10} = 11.37\ \text{kHz} \tag{42}$$

is not listed explicitly in Ref. [11] as a nuclear-spin-dependent contribution to the Lamb shift.

This situation necessitates a few remarks. In Ref. [11], the full Barker-Glover correction, as given in Eq. (25), is included in the atomic-level energies, irrespective of the nuclear spin [i.e., even for deuterium, see Eq. (10) of Ref. [11]]. Still, the absence of the Darwin-Foldy term for deuterium is consistently taken into account in Ref. [11]. Namely, in an earlier paper on CODATA adjustments [see Appendix A8 of Ref. [49], in the text surrounding Eq. (A56)], it is stated that the Darwin-Foldy correction has to be added to the mean-square deuteron radius after all Lamb shift effects have been taken into account. This addition compensates the inclusion of the Darwin-Foldy correction into the deuterium atomic-energy levels [50]. The proton and deuteron charge radii given in Ref. [11] correspond to the conventions used here and in Ref. [2].

To account for a conceivable anomalously large contribution of multiphoton exchange diagrams to the nuclear polarization effect [51], and to accommodate a conceivable large nonlogarithmic part due to the Dirac form factor of the proton, we here add an extra uncertainty of

$$\delta\nu_{11} = 0.5\ \text{kHz}\,, \tag{43}$$

which *replaces* the sum of the uncertainty estimates for $\Delta\nu_7$ and $\Delta\nu_9$ given above in Eqs. (38) and (40). Nevertheless, we cite the uncertainties given in Ref. [11] for the given effects in order to directly relate the discussion to that given in Ref. [11] in a directly reproducible way. The complete result then is

$$\Delta f_{\text{ii}} = \sum_{i=1}^{10} \Delta\nu_i + \delta\nu_{11} = -4502.66(60)\ \text{kHz}\,, \tag{44}$$

where we have added the uncertainties quadratically. This concludes our evaluation of the corrections given by set (ii) according to the classification in Sec. III A.

Set (iii). We now turn to set (iii), which are higher-order nuclear-size corrections to the isotope shift. The general paradigm is as follows. One separates the nuclear-size correction to the hydrogen and deuterium energy levels into a main effect, which is given in Eq. (1) and is directly proportional to the mean-square charge-radius difference. Higher-order corrections to this effect involve higher powers of $Z\alpha$ than four and depend on other details of the nuclear charge distribution such as the third Zemach moment [52–54], in addition to the mean-square charge radius. Numerically, the higher-order corrections are sufficiently small so that they can be evaluated separately, and their uncertainty does not affect the final result for the mean-square charge-radius difference at the current level of accuracy.

The nuclear-finite-size effect is the sum of the following terms: (a) main nonrelativistic effect, (b) third Zemach moment, (c) relativistic corrections, (d) self-energy corrections to the finite-size effect, and (e) vacuum-polarization corrections to the finite-size effect. As already explained, the first of the indicated effects (the main nonrelativistic nuclear-size correction) is already given in Eq. (1) and forms the single entry of set (iv). A very concise discussion of these corrections, together with a list of helpful literature references, is given in Secs. IV A h and IV A i of Ref. [11].

The third Zemach moment correction can be expressed as

$$\begin{aligned} E_{\text{NS,(b)}} &= E_{\text{NS}}\left(-\frac{1}{2}(Z\alpha)\,\frac{m_r}{m_e}\,\frac{\langle r^3\rangle_{(2)}}{\lambda\!\!\!^{-}_C}\,\langle r^2\rangle\right), \\ &= E_{\text{NS}}\left(-C_\eta\,(Z\alpha)\,\frac{m_r}{m_e}\frac{\sqrt{\langle r^2\rangle}}{\lambda\!\!\!^{-}_C}\right), \end{aligned} \tag{45}$$

where the third Zemach moment $\langle r^3\rangle_{(2)}$ is defined in Refs. [52,53], and $\lambda\!\!\!^{-}_C$ is the Compton wavelength of the electron divided by 2π. The parameter

$$C_\eta \equiv \frac{1}{2}\,\frac{\langle r^3\rangle_{(2)}}{\langle r^2\rangle^{3/2}} \tag{46}$$

has been introduced in Eq. (52) of Ref. [11] to express the third Zemach moment as a multiplicative correction to the mean-square charge radius. The value of C_η depends on the shape of the nuclear charge distribution. The deuterium value $C_\eta = 2.0(1)$ for the parameter C_η is taken from Ref. [11]. For hydrogen, we also use the value $C_\eta = 2.0(1)$. This value is consistent with the model-independent determination of the third Zemach moment based on world scattering data, as described in Ref. [52], and also with the reanalysis of the third Zemach moment recently performed in Ref. [54].

According to Ref. [53] and Eq. (52) of Ref. [11], relativistic corrections can be summarized as

$$\begin{aligned} E_{\text{NS,(c)}} = &-E_{\text{NS}}\,(Z\alpha)^2\left[\ln\left(\frac{m_r}{m_e}\frac{\sqrt{\langle r^2\rangle}}{\lambda\!\!\!^{-}_C}\frac{Z\alpha}{n}\right)\right. \\ &\left. + \psi(n) + \gamma_{\text{E}} - \frac{(5n+9)(n-1)}{4n^2} - C_\theta\right]. \end{aligned} \tag{47}$$

Here, according to Ref. [11], the hydrogen value reads as $C_\theta = 0.47(4)$ and the deuterium value is $C_\theta = 0.38(4)$. The self-energy contribution to the nuclear-finite-size correction is

$$E_{\text{NS,(d)}} = \alpha(Z\alpha)\,E_{\text{NS}}\left(4\ln(2) - \frac{23}{4}\right)\delta_{\ell 0}\,. \tag{48}$$

Finally, according to Eq. (55) of Ref. [11], the vacuum-polarization contribution to the nuclear-finite-size correction is an order-α correction to the main nonrelativistic finite-nuclear-size energy E_{NS}:

$$E_{\text{NS,(e)}} = \tfrac{3}{4}\,\alpha(Z\alpha)\,E_{\text{NS}}\,\delta_{\ell 0}. \tag{49}$$

Adding $E_{\text{NS,(b)}} + E_{\text{NS,(c)}} + E_{\text{NS,(d)}} + E_{\text{NS,(e)}}$ and calculating their contribution to the isotope shift, we find

$$\Delta f_{\text{iii}} = -1.73\ \text{kHz} \tag{50}$$

with an uncertainty below 0.01 kHz. $E_{\mathrm{NS,(a)}}$ is the leading-order nuclear-size effect, which directly leads to the mean-square charge-radius difference [see Eq. (1)].

IV. NUCLEAR RADIUS DIFFERENCE

Adding the results reported in Eqs. (28), (44), and (50), we obtain the total theoretical result for the sets of contributions i+ii+iii:

$$\Delta f_{\mathrm{th}} = \Delta f_{\mathrm{i}} + \Delta f_{\mathrm{ii}} + \Delta f_{\mathrm{iii}} = 670\,999\,566.90(66)(60)\ \mathrm{kHz}\,, \tag{51}$$

where the first uncertainty is due to the mass ratios and the second uncertainty is due to nuclear polarization and higher-order quantum electrodynamic (QED) effects. The combined uncertainty is 0.89 kHz. Finally, we arrive at the main nuclear-size correction [Set (iv).], which corresponds to the frequency given in Eq. (1),

$$f_{\mathrm{iv}} = f_{\mathrm{NS}} = \frac{2}{3}\left(\frac{m_r}{m_e}\right)^3 \frac{(Z\alpha)^4 m_e c^2}{h\, n^3} \frac{\langle r^2\rangle}{\lambda\!\!\!^{-}_C{}^2}\,. \tag{52}$$

The isotope-shift frequency corresponding to f_{NS} is Δf_{NS}, as given in Eq. (12). Now, if we evaluate f_{NS} using the charge radii given in Ref. [11] and add all contributions to the isotope shift, we obtain $f_{\mathrm{i+ii+iii+iv}} = 670\,994\,346(23)$ kHz, which is in agreement with the experimental result (9) but much less precise. On the other hand, if we subtract the theoretical result for f_{th} given in Eq. (51) from the experimental result (3), we obtain

$$\Delta f_{\mathrm{NS}} = -5232.29(89)\ \mathrm{kHz} \tag{53}$$

for the contribution to the isotope shift due to the main nuclear-size effect. Solving for the mean-square charge-radii difference with the help of Eq. (52), we obtain

$$\langle r^2\rangle_d - \langle r^2\rangle_p = 3.820\,07(65)\ \mathrm{fm}^2\,. \tag{54}$$

This is more accurate than the corresponding result $\langle r^2\rangle_d - \langle r^2\rangle_p = 3.8212(15)$ fm^2 given in Ref. [2] and also more accurate than the result $\langle r^2\rangle_d - \langle r^2\rangle_p = 3.8213(12)$ fm^2 given in Sec. 16.1.6 of Ref. [10] (where, for the latter result, we have added the individual uncertainties given in Ref. [10] quadratically).

Our value for the deuteron structure radius defined according to Eq. (11) of Ref. [2] is

$$\langle r^2\rangle_{\mathrm{str}} = \langle r^2\rangle_d - \langle r^2\rangle_n - \langle r^2\rangle_p - \frac{3\hbar^2}{4\, m_p^2\, c^2}\,, \tag{55a}$$

$$r_{\mathrm{str}} = 1.975\,07(78)\ \mathrm{fm}\,, \tag{55b}$$

where $\langle r^2\rangle_n = -0.114(3)$ fm^2 is the neutron charge radius [55,56]. The last term on the right-hand side of Eq. (55a) corresponds to the Darwin-Foldy correction for the proton. The connection of the Darwin-Foldy correction to atomic-energy levels, and of the Darwin-Foldy term in the nuclear radius, is explained in Eqs. (26), (27) and (41).

V. CONCLUSIONS

In this paper, we have discussed the essential improvements that have led to an increase in the accuracy of the 1S-2S isotope-shift frequency of the latest measurement [1] as compared to the 1997 measurement [2] (see Sec. II). Contributions to the theoretical expression for the isotope shift have been listed in Sec. III. A detailed account of the corrections that contribute at the current level of accuracy is important as it enables theorists and experimentalists to compare the proton-deuteron radius difference derived from high-precision spectroscopy of hydrogen to scattering data [14–16], based on a transparent listing of theoretical contributions. Finally, in Sec. IV, we derive the nuclear-radius difference of proton and deuteron from the experimental data for the isotope measurement.

The main results of this paper are the deuteron-proton rms charge-radius difference [Eq. (54)] $\langle r^2\rangle_d - \langle r^2\rangle_p = 3.820\,07(65)$ fm^2 as well as the deuteron structure radius $r_{\mathrm{str}} = 1.975\,07(78)$ fm. Moreover, our radius difference (54) is in agreement with the difference of the individual 2006 CODATA values for the proton and deuteron radii [11]. Furthermore, the radius difference derived from our experiment and the 2006 CODATA value of the deuteron radius are in agreement with the proton radius derived from the latest Mainz microtron experiment [17].

The agreement of the deuteron-proton charge-radius difference with the 2006 CODATA values for the individual radii [11] is important for a number of reasons. The primary one is a recent measurement in muonic hydrogen, which has led to a different proton radius or, alternatively, to an interesting disagreement of theory and experiment [3].

ACKNOWLEDGMENTS

Very helpful conversations with P. J. Mohr, J. L. Friar, and I. Sick are gratefully acknowledged. We thank B. Bernhardt, K. Predehl, T. Wilken, and R. Holzwarth for experimental support. U.D.J. acknowledges support from the National Science Foundation (Grant No. PHY–8555454) and from the National Institute of Standards and Technology (Precision Measurement Grant). J.A. acknowledges support from the Marie Curie program of the European Commission, N.K. acknowledges support by the Presidential Grant No. MD-669.2011.8 (Russian Federation), and T.W.H. acknowledges support from the Max Planck Foundation.

[1] C. G. Parthey, A. Matveev, J. Alnis, R. Pohl, T. Udem, U. D. Jentschura, N. Kolachevsky, and T. W. Hänsch, Phys. Rev. Lett. **104**, 233001 (2010).

[2] A. Huber, Th. Udem, B. Gross, J. Reichert, M. Kourogi, K. Pachucki, M. Weitz, and T. W. Hänsch, Phys. Rev. Lett. **80**, 468 (1998).

[3] R. Pohl *et al.*, Nature (London) **466**, 213 (2010).

[4] L. C. Maximon and J. A. Tjon, Phys. Rev. C **62**, 054320 (2000).

[5] M. Vanderhaeghen, J. M. Friedrich, D. Lhuillier, D. Marchand, L. Van Hoorebeke, and J. Van de Wiele, Phys. Rev. C **62**, 025501 (2000).

[6] L. W. Mo and Y. S. Tsai, Rev. Mod. Phys. **41**, 205 (1969).

[7] R. Ent, B. W. Filippone, N. C. R. Makins, R. G. Milner, T. G. O'Neill, and D. A. Wasson, Phys. Rev. C **64**, 054610 (2001).

[8] P. G. Blunden, W. Melnitchouk, and J. A. Tjon, Phys. Rev. C **72**, 034612 (2005).

[9] F. Weissbach, K. Hencken, D. Trautmann, and I. Sick, Phys. Rev. C **80**, 064605 (2009).

[10] M. I. Eides, H. Grotch, and V. A. Shelyuto, Phys. Rep. **342**, 63 (2001).

[11] P. J. Mohr, B. N. Taylor, and D. B. Newell, Rev. Mod. Phys. **80**, 633 (2008).

[12] I. Sick and D. Trautmann, Nucl. Phys. A **637**, 559 (1998).

[13] U. D. Jentschura, S. Kotochigova, E.-O. Le Bigot, P. J. Mohr, and B. N. Taylor, Phys. Rev. Lett. **95**, 163003 (2005).

[14] R. Rosenfelder, Phys. Lett. B **479**, 381 (2000).

[15] I. Sick, Phys. Lett. B **576**, 62 (2003).

[16] I. Sick, Can. J. Phys. **85**, 409 (2007).

[17] J. C. Bernauer *et al.*, Phys. Rev. Lett. **105**, 242001 (2010).

[18] N. Kolachevsky, A. Matveev, J. Alnis, C. G. Parthey, S. G. Karshenboim, and T. W. Hänsch, Phys. Rev. Lett. **102**, 213002 (2009).

[19] N. Kolachevsky, P. Fendel, S. G. Karshenboim, and T. W. Hänsch, Phys. Rev. A **70**, 062503 (2004).

[20] L. Essen, R. W. Donaldson, M. J. Bangham, and E. G. Hope, Nature (London) **229**, 110 (1971).

[21] J. D. Wineland and N. F. Ramsey, Phys. Rev. A **5**, 821 (1972).

[22] M. Haas *et al.*, Phys. Rev. A **73**, 052501 (2006).

[23] A. Huber, B. Gross, M. Weitz, and T. W. Hänsch, Phys. Rev. A **59**, 1844 (1999).

[24] J. Alnis, A. Matveev, N. Kolachevsky, T. Udem, and T. W. Hänsch, Phys. Rev. A **77**, 053809 (2008).

[25] M. Fischer *et al.*, Phys. Rev. Lett. **92**, 230802 (2004).

[26] M. Haas, U. D. Jentschura, and C. H. Keitel, Am. J. Phys. **74**, 77 (2006).

[27] W. A. Barker and F. N. Glover, Phys. Rev. **99**, 317 (1955).

[28] D. Hanneke, S. Fogwell, and G. Gabrielse, Phys. Rev. Lett. **100**, 120801 (2008).

[29] R. Bouchendira, P. Cladé, S. Guellati-Khélifa, F. Nez, and F. Biraben, Phys. Rev. Lett. **106**, 080801 (2011).

[30] J. C. deVries, Ph.D. thesis, Massachusetts Institute of Technology, 2002.

[31] J. Sapirstein and D. R. Yennie, in *Quantum Electrodynamics*, Advanced Series on Directions in High Energy Physics, Vol. 7, edited by T. Kinoshita (World Scientific, Singapore, 1990), pp. 560–672.

[32] V. B. Berestetskii, E. M. Lifshitz, and L. P. Pitaevskii, *Quantum Electrodynamics*, 2nd ed. (Pergamon, Oxford, UK, 1982).

[33] J. L. Friar, J. Martorell, and D. W. L. Sprung, Phys. Rev. A **56**, 4579 (1997).

[34] E. Salpeter, Phys. Rev. **87**, 328 (1952).

[35] A. Czarnecki and K. Melnikov, Phys. Rev. Lett. **87**, 013001 (2001).

[36] M. I. Eides, H. Grotch, and V. A. Shelyuto, Phys. Rev. A **63**, 052509 (2001).

[37] M. I. Eides and H. Grotch, Phys. Rev. A **52**, 1757 (1995).

[38] K. Pachucki, Phys. Rev. A **52**, 1079 (1995).

[39] K. Pachucki and S. G. Karshenboim, Phys. Rev. A **60**, 2792 (1999).

[40] K. Melnikov and A. S. Yelkhovsky, Phys. Lett. B **458**, 143 (1999).

[41] G. Bhatt and H. Grotch, Phys. Rev. A **31**, 2794 (1985).

[42] G. Bhatt and H. Grotch, Phys. Rev. Lett. **58**, 471 (1987).

[43] G. Bhatt and H. Grotch, Ann. Phys. (NY) **178**, 1 (1987).

[44] I. B. Khriplovich and R. A. Senkov, Phys. Lett. A **249**, 474 (1998).

[45] R. Rosenfelder, Phys. Lett. B **463**, 317 (1999).

[46] I. B. Khriplovich and R. A. Senkov, Phys. Lett. B **481**, 447 (2000).

[47] J. L. Friar and G. L. Payne, Phys. Rev. C **56**, 619 (1997).

[48] K. Pachucki and S. G. Karshenboim, J. Phys. B: At., Mol. Opt. Phys. **28**, L221 (1995).

[49] P. J. Mohr and B. N. Taylor, Rev. Mod. Phys. **72**, 351 (2000).

[50] U. D. Jentschura, Eur. Phys. J. D **61**, 7 (2011).

[51] K. Pachucki (private communication).

[52] J. L. Friar and I. Sick, Phys. Rev. A **72**, 040502(R) (2005).

[53] J. L. Friar, Ann. Phys. (NY) **122**, 151 (1979).

[54] M. O. Distler, J. C. Bernauer, and T. Walcher, Phys. Lett. B **693**, 343 (2011).

[55] S. Kopecky, P. Riehs, J. A. Harvey, and N. W. Hill, Phys. Rev. Lett. **74**, 2427 (1995).

[56] S. Kopecky, J. A. Harvey, N. W. Hill, M. Krenn, M. Pernicka, P. Riehs, and S. Steiner, Phys. Rev. C **56**, 2229 (1997).